Reyes-Chaparro *et al.*
Bulletin of the National Research Centre (2023) 47:46
https://doi.org/10.1186/s42269-023-01018-9

Bulletin of the National Research Centre

RESEARCH

Open Access

Design of new reversible and selective inhibitors of monoamine oxidase A and a comparison with drugs already approved

A. Reyes-Chaparro[1], N. S. Flores-Lopez[1], F. Quintanilla-Guerrero[4], Dulce Estefanía Nicolás-Álvarez[2] and A. R. Hernandez-Martinez[1,3,4*]

Abstract

Background Monoamine oxidase (MAO) is an enzyme that has been targeted pharmacologically for the treatment of depression and neurodegenerative diseases such as Parkinson's disease. To avoid side effects, drugs currently in use must selectively target either of the enzyme's two isoforms, A or B. In this study, we designed molecules derived from chalcone as potential reversible and selective inhibitors of isoform A of the MAO enzyme.

Results Ten thousand one hundred compounds were designed and screened using molecular docking, considering the pharmacokinetic processes of chemical absorption, distribution, metabolism, and excretion. Density functional theory calculations were performed for the main ligands to evaluate their reactivity. Six drugs qualified as reversible and irreversible inhibitors of both isoform A and isoform B. Among these, molecule 356 was found to be a reversible inhibitor with the best performance in selectively targeting isoform A of the MAO enzyme. The interaction stability of ligand 356 in the isoform A binding site was confirmed by molecular dynamics. One hydrogen bond was found between the ligand and the cofactor, and up to six hydrogen bonds were formed between the ligand and the protein.

Conclusions We selected a drug model (molecule 356) for its high affinity to isoform A over isoform B of the MAO enzyme. This proposal should decrease experimental costs in drug testing for neurodegenerative diseases. Therefore, our silico design of a reversible inhibitor of isoform A of enzyme monoamine oxidase can be used in further experimental designs of novel drugs with minimal side effects.

Keywords MAO-A, MAO-B, Inhibitor, Reversible, DFT, Molecular docking, Molecular dynamics

*Correspondence:
A. R. Hernandez-Martinez
angel.ramon.hernandez@gmail.com
Full list of author information is available at the end of the article

Graphical Abstract

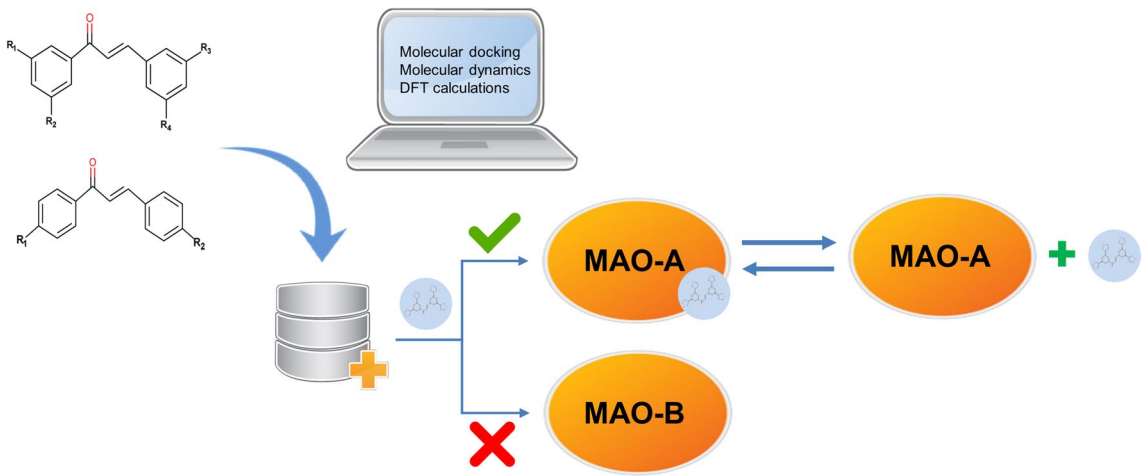

Background

Monoamine oxidase (MAO) has been a pharmacological target for treating depression and neurodegenerative diseases due to its role in regulating the levels of neurotransmitters in the brain. This enzyme (EC 1.4.3.4.) is a flavoenzyme that metabolizes a wide range of primary, secondary, and tertiary monoamines, but has a lower affinity for diamines. MAOis expressed in most body tissues, with the highest levels in the liver (Mardani Moghanaki et al. 2022; Mondovì and Finazzi Agrò 1982; Shih and Lan 1990). It is located on the outer membrane of the mitochondria inside the cell and forms dimers (Denney and Denney 1985; Edmondson et al. 2009; Yelekçi and Erdem 2023). There are two MAO isoforms, MAO-A and MAO-B, encoded by different genes but with 70% coincidence in their amino acid sequence (Finberg 2014; Khan et al. 2022). MAO-A and MAO-B are integral mitochondrial outer membrane proteins and, as isoenzymes, are distinguished from each other by differences in substrates and inhibitor specificities (Finberg 2014). MAO-A is inactivated by the irreversible inhibitor clorgyline, and it oxidizes serotonin, norepinephrine, and epinephrine (Aboutabl et al. 2021), whereas MAO-B is inactivated by the irreversible inhibitors pargyline and selegiline and it oxidizes phenylethylamine and benzylamine. Tyramine and tryptamine are oxidized by both MAO-A and MAO-B. They also have differences in their tissue distribution, e.g., placental tissue contains predominantly MAO-A, while platelets and lymphocytes express only MAO-B (Chen and Shih 1997; Edmondson et al. 2009; Hitge et al. 2022).

Both MAO-A and MAO-B play a critical role in the elimination of neurotransmitters such as norepinephrine, serotonin, and dopamine from the brain. Changes in the activity of these enzymes are linked to various psychiatric pathologies. The study of drugs successfully used for treating severe depression has led to the development of two theoretical models to explain their mechanisms of action, one of which is known as "cerebral monoamine deficiency".

The "cerebral monoamine deficiency" model is shown in Fig. 1. The noradrenergic, serotonergic, and dopaminergic neuronal pathways start in the cerebral cortex expanding toward lower brain structures and modulating mental processes such as thoughts, feelings, and other cognitive activities. Certain antidepressant drugs are known to block the reuptake of monoamines (norepinephrine, serotonin, or dopamine) by presynaptic neurons. This is achieved by inhibiting MAO-A or MAO-B, which are responsible for the degradation of monoamines.

MAO-A inhibitors are effective in decreasing the metabolism of norepinephrine and 5-HT; for this reason they are used as antidepressants, while MAO-B inhibitors are used for the treatment of Parkinson's disease due to their role in dopamine metabolism (Finberg and Rabey 2016). MAO inhibitors can be irreversible or reversible in effect and can be selective for MAO-A or MAO-B. Nevertheless, the use of non-selective and irreversible inhibitors requires dietary restrictions due to serious cardiovascular effects that occur if during treatment, foods containing tyramine are consumed; interactions with those inhibitors have been called "cheese effect" and

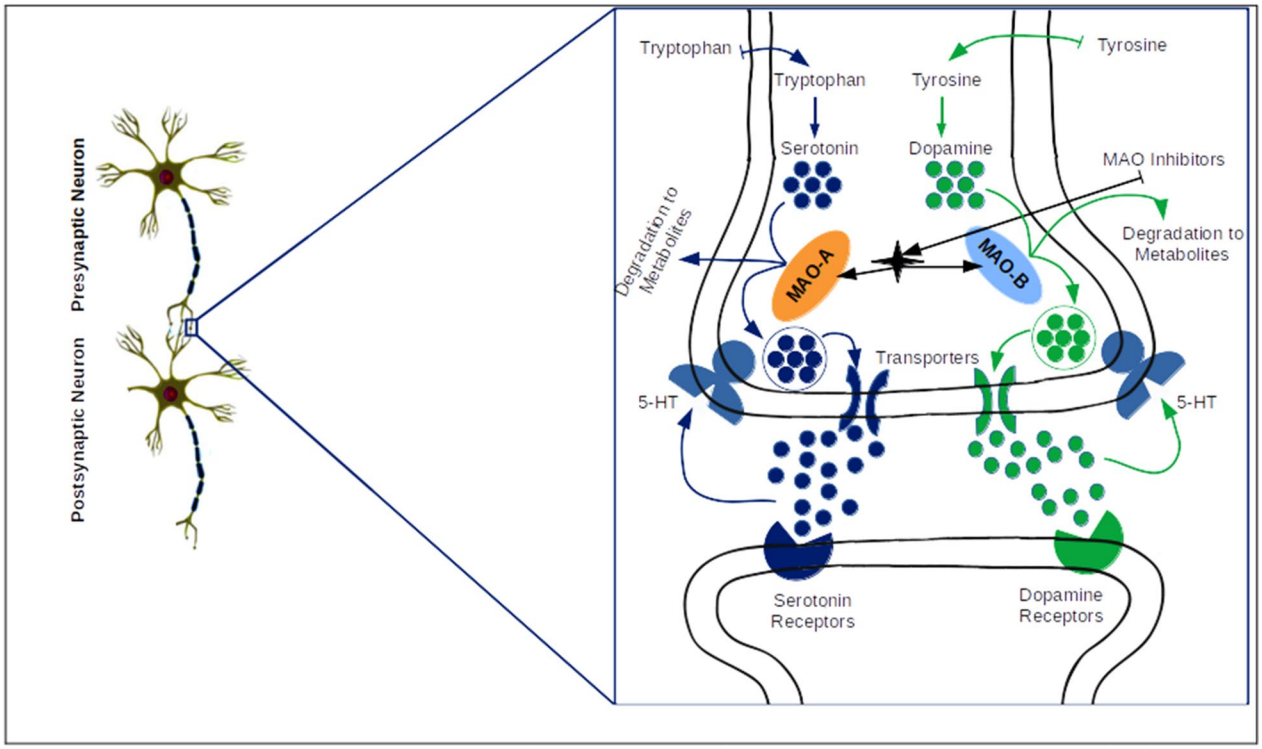

Fig. 1 Simplified schematization of the mechanism of action of monoamine oxidase inhibitors

tyramine is found (in these cases) mainly in sympathetic neurons (Finberg and Gillman 2011; Rendić et al. 2022). It is also reported that the effects of these non-selective and irreversible drugs can result in the suicide of a patient (Finberg 2014). Hence, a selective and reversible inhibition of MAO-A is desirable to treat most depressive disorders.

On the other hand, Computer-aided drug discovery (CADD) is being widely used in the development of new drugs, from pharmaceutical industries to research groups (Medina-Franco 2021). CADD includes various theoretical disciplines such as cheminformatics, bioinformatics, data mining and more recently artificial intelligence (López-López et al. 2021). Molecular docking is a tool that searches for the most feasible binding geometry of a ligand in the 3D space of the receptor active site, positions are scored resulting in interaction strength (Kitchen et al. 2004; Madanagopal et al. 2022). Density functional theory (DFT) reformulates the problem to be able to obtain, for example, the energy and electron distribution of the ground state, working with the electron density functional instead of the wave function (Hoffmann and Rychlewski 2002). With the theory of density functionals, certain molecular descriptors such as chemical potential, hardness, and softness can be rigorously defined and quantified because DFT works with electronic density (LaPointe and Weaver 2007; García-Toral et al. 2022; Zhao et al. 2022).

The use of computational tools in research for new drugs has proven to be highly efficient in terms of cost and benefit, providing new opportunities to increase the precision and effectiveness of the drug development process through in silico methods. This paper presents the results of our research and development efforts focused on designing a new selective and reversible MAO inhibitor drug with fewer side effects using CADD tools. In this regard, an *in silico* design of novel reversible MAO inhibitor drugs was proposed, which could de-absorbed from the substrate by competition effects with serotonin at high concentrations and could prevent the serotonergic syndrome.

Results

A total of 10,100 chalcone-derived molecules were obtained (Additional files 1, 2, and 3); then different screening techniques were used for physicochemical properties, molecular docking, molecular dynamics, and DFT calculations to select the best candidates. Drugs used as MAO-A inhibitors were evaluated as a reference comparison.

Molecular docking and dynamics

The resulting molecules of the chalcone derivatives were selected based on the docking results. The highest affinity energy observed between chalcone derivatives and MAO-A was 13 kcal/mol (Table 1); however, this molecule (335) has also high affinity for MAO-B, which would not allow selectivity. In consequence, the molecule selected was ligand 356 due to its high affinity for MAO-A and low affinity energy for MAO-B, which suggests selective binding properties.

Compound 356 (Fig. 2a) occupies the active site of the MAO-A protein, making it a potential competitive inhibitor (Fig. 2b). Two key interactions were presented as hydrogen bonding between the protein and the ligand; Arg206 and Gly110 (Fig. 2c). The interaction with these two amino acids has been previously reported for other molecules that have been proposed as MAO-A inhibitors (Badavath et al. 2016; Esfahani and Mirzaei 2019; Yusufzai et al. 2018).

The stability of the interaction was corroborated by molecular dynamics (Fig. 3), where it is observed that the root mean square deviation (RMSD) between the protein, the ligand and the cofactor is less than 0.6 nm (Fig. 3a). There is a hydrogen bond between the ligand and the cofactor. Still, it is not stable over time, and up to 6 hydrogen bonds are formed with the ligand and the protein, giving stability to the molecule at the binding site of the protein (Fig. 3b). The root mean square fluctuation (RMSF; Fig. 3c) is a measure of the movement of the atoms of the protein chain; the region with the greatest movement of the MAO-A is the beginning between 1 and 200 atoms. Radius of gyration (Rg) was measured in the entire trajectory, the results show a variation of 0.05 nm (2.32–2.37 nm), which verifies the stability of the tertiary structure of the protein with respect to its center of mass (Fig. 3d). MD results indicate that the interaction between compound 356 and MAO-A is stable and will also have selectivity with respect to MAO-B.

On the other hand, molecular docking studies of the inhibitors show that the affinity energy varies between −6.10 and −8.87 kcal/mol (Table 2). Irreversible inhibitors would be expected to have higher affinity energy than reversible inhibitors. However, the results do not correlate; since moclobemide, a reversible inhibitor has higher affinity energy than irreversible inhibitors. Therefore, the affinity energy result cannot be considered as a measure of the potential reversibility of the proposed compounds. Hence, new studies were proposed using molecular dynamics and DFT calculations.

Table 1 Docking molecular score of chalcone derivatives with MAO-A and MAO-B enzymes

Ligand	MAO-A	MAO-B	Difference
356	−12.9	−8.8	−4.1
541	−12.7	−9.8	−2.9
542	−12.8	−11.1	−1.7
1780	−13.3	−11.7	−1.6
2041	−12.7	−11.3	−1.4
152	−12.6	−11.4	−1.2
33	−12.6	−11.7	−0.9
335	−13	−12.2	−0.8
125	−12.9	−12.1	−0.8
343	−12.6	−11.8	−0.8
1006	−12.8	−12.2	−0.6
1630	−12.7	−12.2	−0.5
154	−12.6	−12.4	−0.2

Assays were performed using Autodock VINA software, values are affinity energy (Kcal/mol)

Density functional theory (DFT) calculations

DFT results were used to evaluate the reactivity of the molecules, in order to select the best candidates that could be reversible inhibitors of MAO-A such as moclobemide. Considering the HOMO–LUMO energy change (ΔE), which has a direct correlation with the rest of the values (Fig. 4), the MAO-A inhibitors can be divided into three groups: pargyline and tranylcypromine with values of 5.9 and 5.8 eV, phenelzine and clorgyline with a ΔE of 4.7 eV, and finally the M30 which has a lower value of 3.1 eV. Moclobemide, which is the reference molecule as a reversible inhibitor, has a lower value than the first two groups, but higher than M30. The HOMO–LUMO energy change is an indicator of the kinetic stability of the molecule. The higher the ΔE, the greater the stability of the molecule; a high reactivity of the molecule is associated with a lower value of ΔE (Luo et al. 2006; Miar et al. 2021).

DFT results analyses of already approved drugs were used as a comparison point. A color gradient was established from red to green, with the most reactive drugs being represented by the red end and the most stable ones by the green end (Table 3).

Ionization potential (I) is the energy required to remove an electron from the ground state of a molecule; if a higher energy is required, it is considered more stable (green). On the other hand, the electron affinity (A) is the energy released when a molecule in its ground state captures an electron; a high value of ionization potential indicates chemical stability (green), while a high value of electron affinity indicates that it is more likely to accept electrons and therefore more unstable (red). The ionization potential has values from 5.6 to 5.77 eV in the MAO-A, except for phenelzine, which has a value of 4.6 eV; no difference is observed in this parameter between

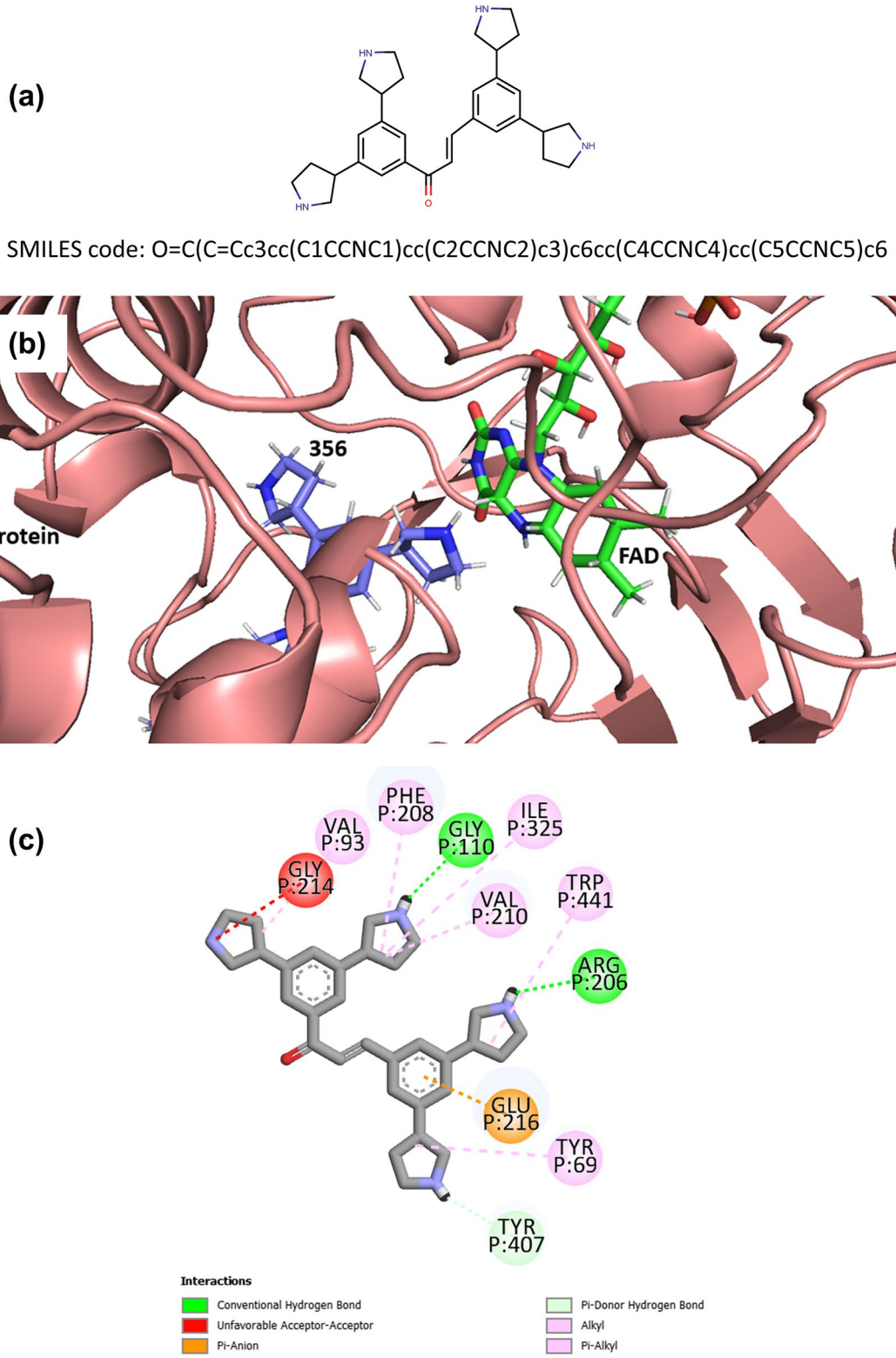

Fig. 2 **a** Molecule 356 and SMILE code; **b** Interaction resulting from molecular docking assays between the 356 ligand and the MAO-A protein; **c** 2D diagram of amino acid interaction

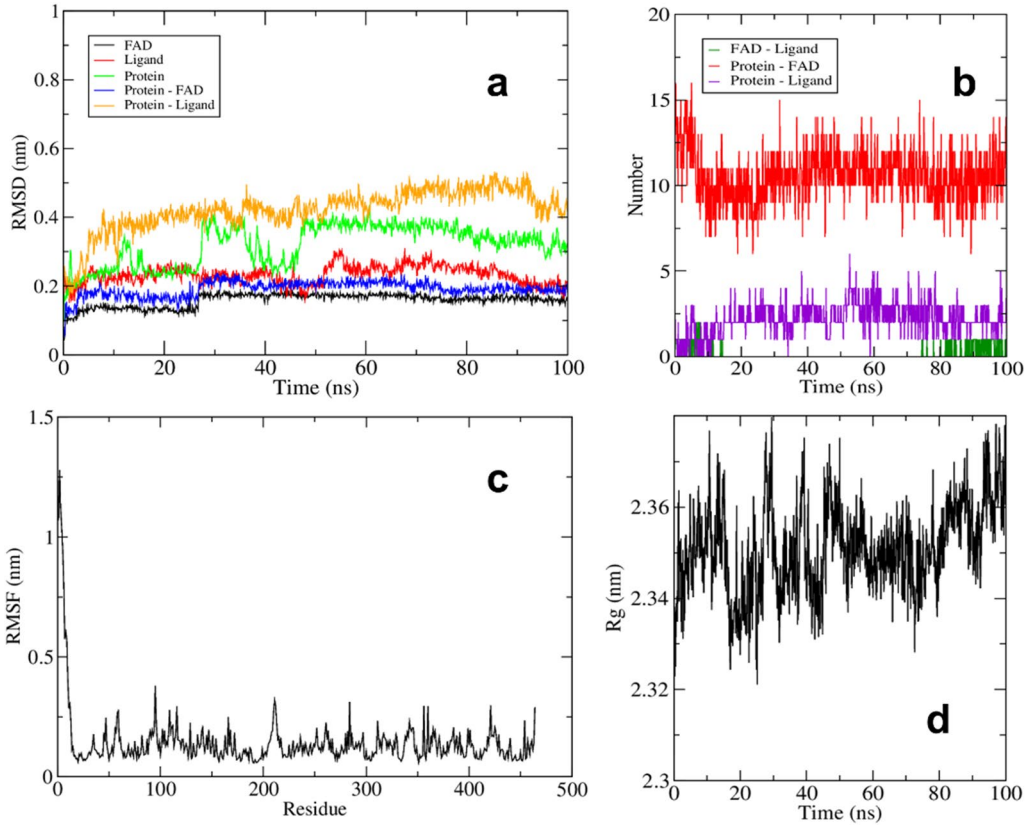

Fig. 3 Molecular dynamics results of the MAO-A receptor ligand-356 complex. **a** RMSD results of each component of the complex; **b** Hydrogen bonds formed between the components of the system; **c** RMSF of the MAO-A; **d** Radius of gyration

Table 2 Molecular docking results of the main commercial drugs used to inhibit MAO-A

Drug	MAO-A	MAO-B	Activity
Tranylcypromine	−6.49 ± 0.05	−6.77 ± 0.099	Irreversible MAO-A + MAO-B
Phenelzine	−6.68 ± 0.05	−6.31 ± 0.052	Irreversible MAO-A + MAO-B
Pargyline	−6.10 ± 0.05	−6.81 ± 0.298	Irreversible MAO-A and MAO-B
Moclobemide	−8.87 ± 0.05	−8.15 ± 0.046	Reversible highly MAO-A selective
M30	−7.85 ± 0.05	−7.63 ± 0.187	MAO-A and MAO-B relative brain selectivity
Clorgiline	−7.24 ± 0.05	−7.02 ± 0.155	Irreversible highly MAO-A selective

Assays were performed using Autodock VINA software, 100 independent assays. Values represent mean ± standard deviation of the energy of affinity (Kcal/mol)

reversible and irreversible inhibitors. While the electronic affinity presents two extremes, from −0.254 to 2.7 eV, leaving moclobemide at an intermediate value of 1.19 eV.

Hardness (η) and softness (σ) are descriptors of the behavior of a molecule in a chemical reaction. Hard molecules have a high resistance to changing their electron distribution during a reaction (higher values are stable, green), while soft molecules have a low resistance to changing their electron distribution during a reaction (lower values are stable, green). As in previous parameters, moclobemide has an intermediate value between the rest of the irreversible inhibitors. It could be considered that a low reactivity also implies that once the covalent bond between flavin adenine dinucleotide (FAD) and the drug is formed, it cannot be easily broken.

The chemical potential (μ) indicates the possibility of a chemical reaction, the high value of μ (less negative) means that it is easier to donate electrons (electron donor), while a small value of μ (more negative) means that it is easier to accept electrons (electron acceptor). Moclobemide and M30 have the highest

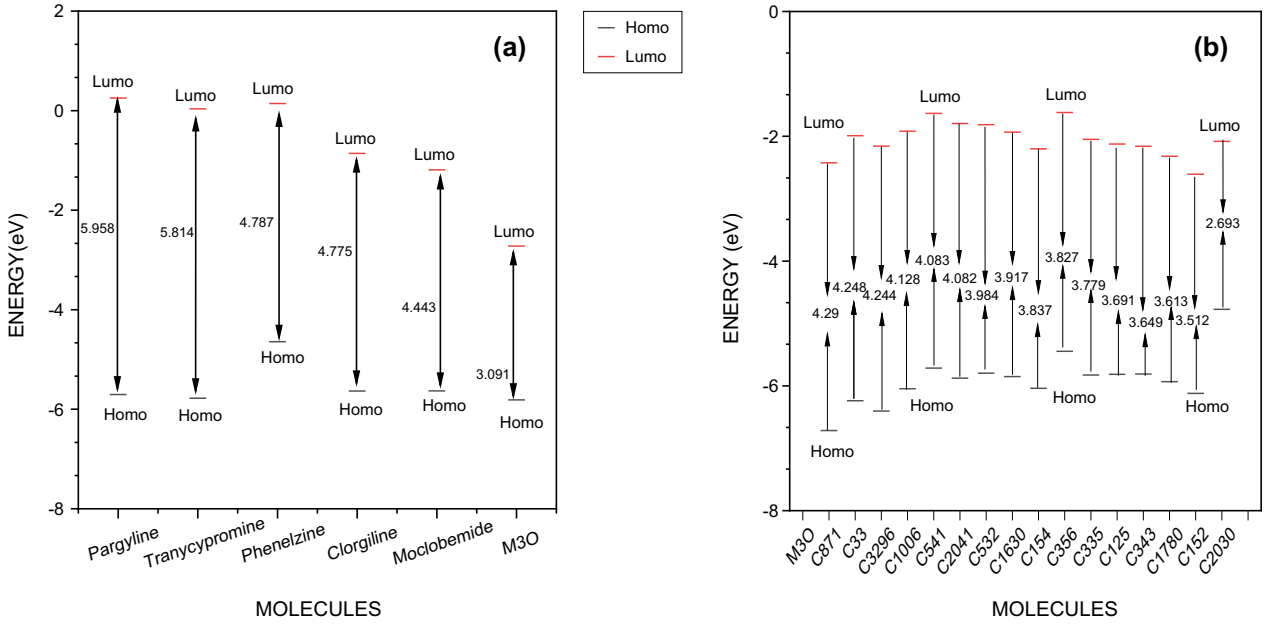

Fig. 4 Molecular orbital diagram, HOMO–LUMO energy change (ΔE); **a** Commercial drugs; and **b** Chalcone derivatives

probability of accepting electrons in a chemical reaction, with the 356 molecules having a chemical potential very close to that of moclobemide, which is the reversible inhibitor.

The electronegativity (χ) of a molecule measures its ability to attract electrons, a lower value is more stable (green). Electrophilicity (ω) is a predictor of the electrophilic nature of a chemical species; measures the propensity of the molecule to accept an electron, with high values of ω they are more reactive (red). The following is a classification of organic molecules based on electrophilicity; weak electrophiles have ω less than 0.8 eV, moderate electrophiles have ω in the range between 0.8 and 1.5 eV, and strong electrophiles have ω greater than 1.5 eV (Edim et al. 2021). Based on this classification, pargyline, phenelzine, and tranylcypromine are moderate electrophiles, and all other molecules are strong electrophiles. The highest values of electronegativity and electrophilic are for drug M30, which presented different values from the rest of the drugs.

In brief, molecule 356 was the best candidate to inhibit MAO-A, due to its high affinity for MAO-A (− 12.9 kcal/mol), and low affinity energy for MAO-B (− 8.8 kcal/mol), which indicates good selectivity. Additionally, molecule 356 presents electronic characteristics and values of medium reactivity similar to moclobemide, considering M30 as a more reactive molecule and pargyline as a more stable molecule.

Discussion

Chalcone derivatives have served as the central nucleus for the design of drugs such as antimicrobials (Guo et al. 2019), anticancer (Ouyang et al. 2021), and anti-inflammatories (Amir et al. 2022), among others (Duran et al. 2021; Weyesa et al. 2021). Proposals for chalcone derivatives as MAO-B inhibitors have been made using coumarin conjugates (Moya-Alvarado et al. 2021), ethoxylated derivatives (Maliyakkal et al. 2022), aldoxime and hydroxy functionalized (Oh et al. 2022). MAO-A inhibitors derived from chalcone have also been designed and they have activity as antidepressants (at a dose of 100 mg/kg) and selectivity for this isoform A (Tan et al. 2022). Chalcone's pharmacological and pharmacokinetic properties can be modified by introducing different substituents on either of its two rings or by attaching other biologically active functional groups (Gomes et al. 2017). These chalcone derivatives features have prompted our decision of selecting these compounds for studying viable drugs to treat neurodegenerative disorders.

We obtained the new molecules considering that the MAO-A active site is hydrophobic, and it has a different shape from MAO-B. MAO-A active site allows larger molecules to interact with the FAD (flavin adenine dinucleotide) cofactor for not having a constriction (tunnel) (Ramsay et al. 2020; Maršavelski et al. 2022).

Irreversible inhibition occurs due to the formation of a covalent bond between the inhibitor and FAD. For example, tranylcypromine forms an adduct at C4a

Table 3 DFT results of MAO-A inhibitors and new molecules

Drug	I	A	η	σ	X	μ	Ω
Pargyline	5.704	−0.254	2.979	0.336	2.725	−2.725	1.247
Tranylcypromine	5.777	−0.036	2.907	0.344	2.870	−2.870	1.417
Phenelzine	4.644	−0.143	2.394	0.418	2.251	−2.251	1.058
Clorgiline	5.635	0.860	2.387	0.419	3.248	−3.248	2.209
Moclobemide	5.631	1.189	2.221	0.450	3.410	−3.410	2.618
M3O	5.811	2.720	1.545	0.647	4.265	−4.265	5.886
				New molecules			
871	6.716	2.426	2.145	0.466	4.571	−4.571	4.871
33	6.239	1.990	2.124	0.471	4.114	−4.114	3.985
3296	6.403	2.159	2.122	0.471	4.281	−4.281	4.318
1006	6.045	1.917	2.064	0.484	3.981	−3.981	3.838
541	5.716	1.633	2.042	0.490	3.675	−3.675	3.307
2041	5.877	1.795	2.041	0.490	3.836	−3.836	3.605
532	5.796	1.813	1.992	0.502	3.805	−3.805	3.634
1630	5.851	1.934	1.959	0.511	3.892	−3.892	3.868
154	6.038	2.201	1.918	0.521	4.120	−4.120	4.423
356	5.445	1.618	1.914	0.523	3.531	−3.531	3.258
335	5.827	2.049	1.889	0.529	3.938	−3.938	4.104
125	5.816	2.125	1.846	0.542	3.971	−3.971	4.271
343	5.810	2.161	1.824	0.548	3.985	−3.985	4.353
1780	5.933	2.320	1.806	0.554	4.126	−4.126	4.713
152	6.121	2.609	1.756	0.570	4.365	−4.365	5.425
2030	4.773	2.080	1.347	0.743	3.427	−3.427	4.360

All values are in eV. Gradient color is based on the stability, where green is the most stable and red the most reactive. Results were calculated using Eqs. 1, 2, 3, 4, 5, 6, 7 and 8.

(Bonivento et al. 2010; Ramsay et al. 2020), while phenelzine, pargyline, clorgyline, selegiline, and rasagiline form adducts on N5 (Binda et al. 2002, 2004, 2008; De Colibus et al. 2005). Some studies determined that the interaction of inhibitors with the FAD cofactor should be a reversible interaction in drug design (Binda et al. 2005; Borštnar et al. 2011; Ganesan 2018; Mardani Moghanaki et al. 2022). Our results indicate that a covalent bond will not be formed as there is no stable interaction between the ligand and the FAD.

Irreversible inhibitors are expected to have higher affinity energy than reversible inhibitors. However, moclobemide was the drug with the highest affinity energy for MAO-A with respect to MAO-B (0.72 kcal/mol), and this is a selective reversible inhibitor (Haefely et al. 1992; Kumar et al. 2022). Therefore, we did not consider the affinity energy as a measure of the potential reversibility of the proposed compounds. To address this issue, we proposed a complete study using molecular dynamics and DFT calculations. Although MAO-A irreversible inhibitors have been reported to be more effective than antidepressants, side effects represent a health problem, so inhibitors such as moclobemide are more recommended (Shulman et al. 2013).

Various studies indicate that molecular docking results coincide with experimental selectivity of the affinity of inhibitors between MAO-A and MAO-B (Chaurasiya et al. 2019; Larit et al. 2018; Yelekçi et al. 2007).

The analysis of our docking results indicates that compound 356 occupies the active site of the MAO-A protein and therefore could be a potential competitive inhibitor, as mentioned in the results section. The stability of the interaction of compound 356 was corroborated by molecular dynamics and the results indicate that the interaction between compound 356 and MAO-A is stable and will also have selectivity with respect to MAO-B. Indicating that this molecule has potential as a component in a drug design for its inhibitory activity of MAO-A, and for being selective and reversible.

The comparison of our proposed compound with inhibitors of MAO-A and MAO-B currently used such as pargyline, tranylcypromine, phenelzine, clorgiline, moclobemide and M30 indicates that compound 356 has medium stability, with similar behavior with moclobemide. Therefore, this study allows the possibility for an in vitro and in vivo evaluation. Computational studies such as ours can enhance the generation of new drugs because they are inexpensive compared with experimental studies for each molecule.

Conclusions

In this study, a library of 10,100 compounds was generated and screened using bioinformatic tools to obtain the best molecule to selectively and reversibly inhibit MAO-A. Molecule 356 showed the best characteristics of high affinity for MAO-A with respect to MAO-B, stability in the binding site and electronic characteristics that will allow it to be a reversible inhibitor. The feature of being a reversible inhibitor could minimize the side effects of the drug, because it may not interfere with enzyme's function when monoamine concentrations are low This proposal should decrease experimental costs in drug testing for neurodegenerative diseases. Therefore, our *in silico* design of a reversible inhibitor of isoform A of enzyme monoamine oxidase can be used in further experimental designs of novel drugs with minimal side effects.

Methods

Chalcone backbone was used as the starting structure to perform different substitutions with R groups at *para* and *meta* positions (Fig. 5A, B, respectively). Ten different R groups were used as substituents (Fig. 5C), from three pharmacophoric groups: hydrophobic, hydrogen bond donors and acceptors. The SMILIB software (Schüller et al. 2007) was used and 100 molecules (resulting from substitutions in *para*) and 10,000 molecules (from substitutions in *meta)* were obtained in *SMILES* code. Both resulting databases (10,100 compounds) were opened in DataWarrior software (Sander et al. 2015; Yang et al. 2019), where they were screened using the following criteria: ≤ 5 hydrogen bond donors, ≤ 10 hydrogen bond acceptors, molecular weight ≤ 500 Da, and cLogP ≤ 5. Obtaining a resulting database of 3321 molecules. 3D coordinates of the resulting molecules were constructed using OpenBabel software (O'Boyle et al. 2011) and transformed into *pdbqt* format.

Molecular docking assays were performed to select the best ligands. Crystallized MAO-A protein (code 2BXR) was downloaded, UCSF Chimera software was used to clean the protein and add polar hydrogens, only FAD cofactor was preserved (Pettersen et al. 2004). Using AutoDock Tools software, the protein was converted to *pdbqt* format, and the grid coordinates for directed docking with AutoDock VINA were generated, and virtual screening was performed using bash scripting (Jaghoori et al. 2016; Trott and Olson 2010). The 100 molecules with the highest affinity energy were selected and molecular docking assays were performed with MAO-B (code 2V5Z), selecting the 10 molecules with the greatest difference between the affinity energy of both enzymes

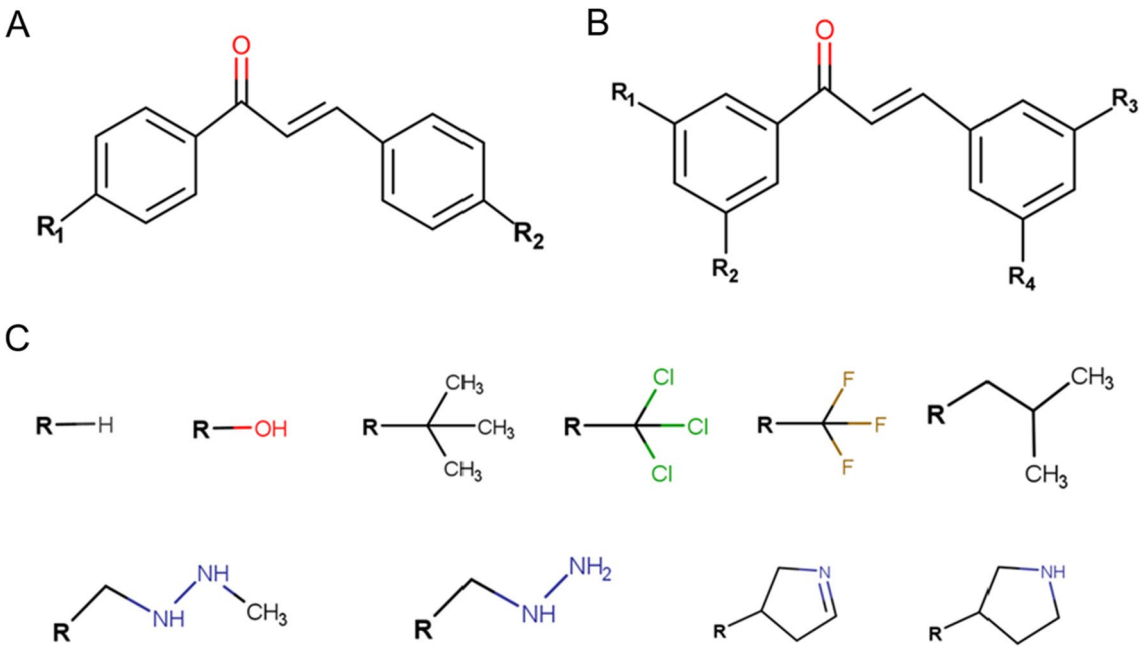

Fig. 5 Developmental components of chalcone derivatives. **A** Substitution of chalcone in *para* sites of benzene rings. **B** Substitution in *meta* sites. **C** Substituents used in both substitution schemes. Images generated using MarvinSketch

(Table 1). For comparison purposes, molecular docking was performed with the common drugs used as MAO-A inhibitors, with the enzymes MAO-A and MAO-B (Table 2) (Happe 2007).

Molecular dynamics tests were carried out to evaluate the stability of the ligand-receptor complexes that resulted from the molecular docking tests. Charmm-gui platform was used to prepare the different inputs, and the Gromacs 2021.1 software for molecular dynamics (Abraham et al. 2015; Jo et al. 2008; Lindahl et al. 2021; Kutzner 2022). Each protein was preprocessed using the PDB reader tool (Jo et al. 2014). On the other hand, the resulting docking ligands with the highest affinity energy were selected and changed to mol2 format using OpenBabel (O'Boyle et al. 2011). The "mol2" files of the ligands were loaded into the Ligand Reader & Modeler tool to generate the parameters and topology files (Kim et al. 2017). The ligand-receptor complexes were integrated into a single. *pdb* file to be used in the "Solution Builder" tool to create the system that was used as input for Gromacs (Lee et al. 2016). Water box was cubic, fit to protein size, and 10 Å of edge distance. Each system was neutralized using KCl ions placed by Monte-Carlo method, at concentration of 0.15 M. Each system underwent 5000 steps of steepest descents energy minimization to remove steric overlap. Afterward, all the systems were subjected to a NVT (constant number of particles, volume and temperature) equilibration phase for 125,000 steps, using the V-rescale temperature-coupling method, with constant coupling of 1 ps at 303.15 K (Bussi et al. 2007). Subsequently, the molecular dynamics was carried out for 100 ns using the CHARMM36m force field (Vanommeslaeghe et al. 2010). Trajectory Analysis: Gromacs utilities were used to evaluate the root mean square deviation (RMSD) of the complexes, as well as that of each protein and ligand, root mean square fluctuation (RMSF), and hydrogen bonds. The data were graphed using the GRACE program.

DFT calculations were performed using Gaussian 09 software. *GaussView* 5.0.8 graphical interface was used to design the molecules (Frisch et al. 2016). Subsequently, calculations and optimization were made using the Becke-3 Parameter-Lee–Yang–Parr (B3LYP) model and the base 6-31G to optimize the best conformation of the molecules (Runge & Gross 1984). First step was the optimization of the geometric structures and vibrational frequencies in search of a minimum of local energy, which is corroborated by verifying that the frequencies presented in the calculation are not negative. Next, the ionic energy and cationic energy calculations for the minimum energy structures were performed. Finally, the electronic energies, ionization potentials, electronic affinity, hardness, and softness for each molecule were obtained.

Quantum calculations allow us to understand the stability of molecules and their chemical reactivity. Koopmans developed a theorem to relate the chemical activities of molecular structures to their electronic properties (Luo

et al. 2006). Quantum chemical descriptors derived from Koopman theorem: ionization potential (I), electron affinity (A), hardness (η), softness (σ), chemical potential (μ), electronegativity (X), and electrophilicity (ω). These parameters are derived from HOMO energy and LUMO energy calculations that are mathematically defined below:

Equations 1–8:

$$\Delta E = E_{\mathrm{LUMO}} - E_{\mathrm{HOMO}} \tag{1}$$

$$I = -E_{\mathrm{HOMO}} \tag{2}$$

$$A = -E_{\mathrm{LUMO}} \tag{3}$$

$$\eta = \frac{I - A}{2} \tag{4}$$

$$\sigma = \frac{1}{\eta} = \frac{I - A}{2} \tag{5}$$

$$X = \frac{I + A}{2} \tag{6}$$

$$\mu = -X \tag{7}$$

$$\omega = \frac{X^2}{2\eta} \tag{8}$$

Abbreviations

MAO	Enzyme monoamine oxidase
MAO-A	Enzyme monoamine oxidase isoform A
MAO-B	Enzyme monoamine oxidase isoform B
DFT	Density functional theory
CADD	Computer-aided drug discovery
RMSD	Root mean square deviation
RMSF	Root mean square fluctuation
FAD	Flavin adenine dinucleotide, redox cofactor

Supplementary Information

The online version contains supplementary material available at https://doi.org/10.1186/s42269-023-01018-9.

Additional file 1. Route 1 of molecule 356 retrosynthesis proposal obtained with SciFinder.

Additional file 2. Route 2 of molecule 356 retrosynthesis proposal obtained with SciFinder.

Additional file 3. SMILIB compounds full data_base.

Acknowledgements

The authors are grateful to CONACYT Frontiers of Science Project No. 845101, "Accelerated Discovery of Antifouling Materials (ADAM)" for their financial and technical support. Karla Gabriela Montes Rangel and Sebastian García Perez for their support in validating some bibliographic data. The computational resources for this investigation were facilitated by UNISON/Acarus. And the support from Luis Aguilar, Alejandro De León, and Jair García of the Laboratorio Nacional de Visualización Científica Avanzada, UNAM. Special gratitude to Ana L. Ramos-Jacques at Edit Academy for her assistance in editing and proofreading the manuscript.

Author contributions

RCA and NADE performed and analyzed the Molecular docking results regarding the enzymes; RCA was a major contributor in writing the manuscript. FLNS performed and analyzed the DFT results. QGF contributed to and supported the process of conceptualization of the research, contributing critical questions to formulate the research problem, as well as reviewing and analyzing the overall results of the report. HMAR was responsible for the conceptualization, management, and supervision of the activities of the research group; He defined the objectives and hypothesis, specified the research, prioritizing the scope of the project, and placed the reasoning behind the research approach. All authors reviewed and approved the collection methods and analysis methods. All authors read and approved the final manuscript.

Funding

This research received no specific grant from any funding agency in the commercial, or not-for-profit sectors.

Availability of data and materials

Data generated or analyzed during this study are included in this published article and its Additional files 1, 2 and 3.

Declarations

Ethics approval and consent to participate

No applicable.

Consent for publication

No applicable.

Competing interests

The authors declare that they have no competing interests.

Author details

[1]Centro de Física Aplicada y Tecnología Avanzada (CFATA), Universidad Nacional Autónoma de México (UNAM), Blvd. Juriquilla 3000, Querétaro, México. [2]Departamento de Fisiología, Escuela Nacional de Ciencia Biológicas (ENCB) del Instituto Politécnico Nacional, Av. Wilfrido Massieu Esq. Cda. Miguel Stampa S/N, Gustavo A. Madero, 07738 Mexico City, México. [3]Instituto de Ingeniería, Universidad Nacional Autónoma de México (UNAM), Circuito Escolar, Ingeniería s/n. Ciudad Universitaria, Coyoacán, 04510 Mexico City, México. [4]Facultad de Química, Universidad Autónoma de Querétaro, Centro Universitario, Cerro de Las Campanas, 76010 Querétaro, México.

Received: 8 November 2022 Accepted: 13 March 2023
Published online: 22 March 2023

References

Aboutabl ME, Salman AM, Gamal el Din AA, Maklad YA (2021) Simultaneous administration of coffee and rasagiline/l-dopa protects against paraquat-induced neurochemical and motor behavior impairments in vivo. Bull Natl Res Cent 45(1):1–20. https://doi.org/10.1186/s42269-021-00678-9

Abraham MJ, Murtola T, Schulz R, Páll S, Smith JC, Hess B, Lindah E (2015) Gromacs: high performance molecular simulations through multi-level parallelism from laptops to supercomputers. SoftwareX 1–2:19–25. https://doi.org/10.1016/j.softx.2015.06.001

Amir M, Verma JS, Tariq S, Somakala K, Ehtaishamul Haq S (2022) Synthesis and biological evaluation of some new chalcone derivatives as anti-inflammatory agents. Curr Drug Discov Technol 57B(7):955–959. https://doi.org/10.2174/1570163819666220613153225

Badavath VN, Baysal I, Ucar G, Sinha BN, Jayaprakash V (2016) Monoamine oxidase inhibitory activity of novel pyrazoline analogues: curcumin based design and synthesis. ACS Med Chem Lett 7(1):56–61. https://doi.org/10.1021/ACSMEDCHEMLETT.5B00326

Binda C, Hubálek F, Li M, Herzig Y, Sterling J, Edmondson DE, Mattevi A (2004) Crystal structures of monoamine oxidase B in complex with four inhibitors of the N-propargylaminoindan class. J Med Chem 47(7):1767–1774. https://doi.org/10.1021/JM031087C

Binda C, Hubálek F, Li M, Herzig Y, Sterling J, Edmondson DE, Mattevi A (2005) Binding of rasagiline-related inhibitors to human monoamine oxidases: a kinetic and crystallographic analysis. J Med Chem 48(26):8148. https://doi.org/10.1021/JM0506266

Binda C, Newton-Vinson P, Hubálek F, Edmondson DE, Mattevi A (2002) Structure of human monoamine oxidase B, a drug target for the treatment of neurological disorders. Nat Struct Biol 9(1):22–26. https://doi.org/10.1038/NSB732

Binda C, Wang J, Li M, Hubalek F, Mattevi A, Edmondson DE (2008) Structural and mechanistic studies of arylalkylhydrazine inhibition of human monoamine oxidases A and B. Biochemistry 47(20):5616–5625. https://doi.org/10.1021/BI8002814/ASSET/IMAGES/MEDIUM/BI-2008-002814_0010.GIF

Bonivento D, Milczek EM, McDonald GR, Binda C, Holt A, Edmondson DE, Mattevi A (2010) Potentiation of ligand binding through cooperative effects in monoamine oxidase B. J Biol Chem 285(47):36849. https://doi.org/10.1074/JBC.M110.169482

Borštnar R, Repič M, Kržan M, Mavri J, Vianello R (2011) Irreversible inhibition of monoamine oxidase B by the antiparkinsonian medicines rasagiline and selegiline: a computational study. Eur J Org Chem 2011(32):6419–6433. https://doi.org/10.1002/EJOC.201100873

Bussi G, Donadio D, Parrinello M (2007) Canonical sampling through velocity rescaling. J Chem Phys. https://doi.org/10.1063/1.2408420

Chaurasiya ND, Zhao J, Pandey P, Doerksen RJ, Muhammad I, Tekwani BL (2019) Selective Inhibition of Human Monoamine Oxidase B by Acacetin 7-Methyl Ether Isolated from Turnera diffusa (Damiana). Molecules 24(4):810. https://doi.org/10.3390/molecules24040810

Chen K, Shih JC (1997) Monoamine oxidase A and B: structure, function, and behavior. Adv Pharmacol 42(C):292–296. https://doi.org/10.1016/S1054-3589(08)60747-4

De Colibus L, Li M, Binda C, Lustig A, Edmondson DE, Mattevi A (2005) Three-dimensional structure of human monoamine oxidase A (MAO A): relation to the structures of rat MAO A and human MAO B. Proc Natl Acad Sci USA 102(36):12684–12689. https://doi.org/10.1073/PNAS.0505975102

Denney RM, Denney CB (1985) An update on the identity crisis of monoamine oxidase: new and old evidence for the independence of mao A and B. Pharmacol Ther 30(3):227–258. https://doi.org/10.1016/0163-7258(85)90050-6

Duran N, Polat MF, Aktas DA, Alagoz MA, Ay E, Cimen F, Tek E, Anil B, Burmaoglu S, Algul O (2021) New chalcone derivatives as effective against SARS-CoV-2 agent. Int J Clin Pract. https://doi.org/10.1111/IJCP.14846

Edim MM, Enudi OC, Asuquo BB, Louis H, Bisong EA, Agwupuye JA, Chioma AG, Odey JO, Joseph I, Bassey FI (2021) Aromaticity indices, electronic structural properties, and fuzzy atomic space investigations of naphthalene and its aza-derivatives. Heliyon 7(2):e06138. https://doi.org/10.1016/J.HELIYON.2021.E06138

Edmondson DE, Binda C, Wang J, Upadhyay AK, Mattevi A (2009) Molecular and mechanistic properties of the membrane-bound mitochondrial monoamine oxidases. Biochemistry 48(20):4220. https://doi.org/10.1021/BI900413G

Esfahani AN, Mirzaei M (2019) Flavonoid derivatives for monoamine oxidase–a inhibition. Adv J Chem Sect B Nat Prod Med Chem 1(1):17–22. https://doi.org/10.33945/SAMI/AJCB.2019.1.4

Finberg JPM (2014) Update on the pharmacology of selective inhibitors of MAO-A and MAO-B: focus on modulation of CNS monoamine neurotransmitter release. Pharmacol Ther 143(2):133–152. https://doi.org/10.1016/j.pharmthera.2014.02.010

Finberg JPM, Gillman K (2011) Selective inhibitors of monoamine oxidase type B and the "cheese effect." Int Rev Neurobiol 100:169–190. https://doi.org/10.1016/B978-0-12-386467-3.00009-1

Finberg JPM, Rabey JM (2016) Inhibitors of MAO-A and MAO-B in psychiatry and neurology. Front Pharmacol. https://doi.org/10.3389/FPHAR.2016.00340

Frisch MJ, Trucks GW, Schlegel HB, Scuseria GE, Robb MA, Cheeseman JR, Scalmani G, Barone V, Petersson GA, Nakatsuji H, Li X, Caricato M, Marenich AV, Bloino J, Janesko BG, Gomperts R, Mennucci B, Hratchian HP, Ortiz JV, Fox DJ (2016) G16_C01 (p. Gaussian 16, Revision C.01, Gaussian, Inc., Wallin).

Ganesan A (2018) Epigenetic drug discovery: a success story for cofactor interference. Philos Trans R Soc B Biol Sci 373(1748):20170069. https://doi.org/10.1098/rstb.2017.0069

García-Toral D, Mendoza-Báez R, Chigo-Anota E, Flores-Riveros A, Vázquez-Báez VM, Cocoletzi GH, Rivas-Silva JF (2022) Structural stability and electronic properties of boron phosphide nanotubes: a density functional theory perspective. Symmetry 14(5):964. https://doi.org/10.3390/sym14050964

Gomes MN, Muratov EN, Pereira M, Peixoto JC, Rosseto LP, Cravo PVL, Andrade CH, Neves BJ (2017) Chalcone derivatives: promising starting points for drug design. Molecules. https://doi.org/10.3390/MOLECULES22081210

Guo T, Xia R, Chen M, He J, Su S, Liu L, Li X, Xue W (2019) Biological activity evaluation and action mechanism of chalcone derivatives containing thiophene sulfonate. RSC Adv 9(43):24942–24950. https://doi.org/10.1039/C9RA05349B

Haefely W, Burkard WP, Cesura AM, Kettler R, Lorez HP, Martin JR, Richards JG, Scherschlicht R, Da Prada M (1992) Biochemistry and pharmacology of moclobemide, a prototype RIMA. Psychopharmacology 10:6. https://doi.org/10.1007/BF02246225

Happe K (2007) Monoamine oxidase inhibitors. xPharm Compr Pharmacol Ref. https://doi.org/10.1016/B978-008055232-3.61002-5

Hitge R, Petzer JP, Petzer A (2022) The inhibition of monoamine oxidase by 2H–1, 4-benzothiazin-3 (4H)-ones. Bioorg Med Chem Lett. https://doi.org/10.1016/j.bmcl.2022.129038

Hoffmann M, Rychlewski J (2002) Density functional theory (DFT) and drug design. Rev Mod Quantum Chem. https://doi.org/10.1142/9789812775702_0058

Jaghoori MM, Bleijlevens B, Olabarriaga SD (2016) 1001 ways to run AutoDock vina for virtual screening. J Comput Aided Mol Des 30(3):237–249. https://doi.org/10.1007/s10822-016-9900-9

Jo S, Cheng X, Islam SM, Huang L, Rui H, Zhu A, Lee HS, Qi Y, Han W, Vanommeslaeghe K, Mackerell AD, Benoit R, Im W (2014) CHARMM-GUI PDB manipulator for advanced modeling and simulations of proteins containing non-standard residues. Adv Protein Chem Struct Biol 96:235–265. https://doi.org/10.1016/bs.apcsb.2014.06.002

Jo S, Kim T, Iyer VG, Im W (2008) CHARMM-GUI: a web-based graphical user interface for CHARMM. J Comput Chem 29:174–182. https://doi.org/10.1002/jcc

Khan BA, Ashfaq M, Muhammad S, Munawar KS, Tahir MN, Al-Sehemi AG, Alarfaji SS (2022) Exploring highly functionalized tetrahydropyridine as a dual inhibitor of monoamine oxidase a and b: synthesis, structural analysis, single crystal XRD, supramolecular assembly exploration by hirshfeld surface analysis, and computational studies. ACS Omega 7(33):29452–29464. https://doi.org/10.1021/acsomega.2c03909

Kim S, Lee J, Jo S, Brooks CL, Lee HS, Im W (2017) CHARMM-GUI ligand reader and modeler for CHARMM force field generation of small molecules. J Comput Chem 38(21):1879–1886. https://doi.org/10.1002/jcc.24829

Kitchen DB, Decornez H, Furr JR, Bajorath J (2004) Docking and scoring in virtual screening for drug discovery: methods and applications. Nat Rev Drug Discov 3(11):935–949. https://doi.org/10.1038/nrd1549

Kumar A, Bhatia M, Kapoor A, Kumar P, Kumar S (2022) Monoamine oxidase inhibitors: a concise review with special emphasis on structure activity relationship studies. Eur J Med Chem. https://doi.org/10.1016/j.ejmech.2022.114655

Kutzner C, Kniep C, Cherian A, Nordstrom L, Grubmüller H, de Groot BL, Gapsys V (2022) GROMACS in the cloud: a global supercomputer to speed up alchemical drug design. J Chem Inf Model 62(7):1691–1711. https://doi.org/10.1021/acs.jcim.2c00044

LaPointe SM, Weaver DF (2007) A review of density functional theory quantum mechanics as applied to pharmaceutically relevant systems. Curr Comput Aided-Drug Des 3(4):290–296. https://doi.org/10.2174/157340907782799390

Larit F, Elokely KM, Chaurasiya ND, Benyahia S, Nael MA, León F, Abu-Darwish MS, Efferth T, Wang YH, Belouahem-Abed D, Benayache S, Tekwani BL, Cutler SJ (2018) Inhibition of human monoamine oxidase A and B by flavonoids isolated from two Algerian medicinal plants. Phytomedicine 40:27–36. https://doi.org/10.1016/j.phymed.2017.12.032

Lee J, Cheng X, Swails JM, Yeom MS, Eastman PK, Lemkul JA, Wei S, Buckner J, Jeong JC, Qi Y, Jo S, Pande VS, Case DA, Brooks CL, MacKerell AD, Klauda JB, Im W (2016) CHARMM-GUI input generator for NAMD, GROMACS, AMBER, OpenMM, and CHARMM/OpenMM simulations using the

CHARMM36 additive force field. J Chem Theory Comput 12(1):405–413. https://doi.org/10.1021/acs.jctc.5b00935
Lindahl, Abraham, Hess, & Spoel van der (2021) GROMACS 2021 Source code. Doi: 10.5281/ZENODO.4457591
Luo J, Xue ZQ, Liu WM, Wu JL, Yang ZQ (2006) Koopmans' theorem for large molecular systems within density functional theory. J Phys Chem A 110(43):12005–12009. https://doi.org/10.1021/JP063669M
López-López E, Bajorath J, Medina-Franco JL (2021) Informatics for chemistry, biology, and biomedical sciences. J Chem Inf Model 61(1):26–35. https://doi.org/10.1021/ACS.JCIM.0C01301/SUPPL_FILE/CI0C01301_SI_001.PDF
Madanagopal P, Ramprabhu N, Jagadeesan R (2022) In silico prediction and structure-based multitargeted molecular docking analysis of selected bioactive compounds against mucormycosis. Bull Natl Res Cent 46(1):1–21. https://doi.org/10.1186/s42269-022-00704-4
Maliyakkal N, Saleem U, Anwar F, Shah MA, Ahmad B, Umer F, Almoyad MAA, Parambi DGT, Beeran AA, Nath LR, Aleya L, Mathew B (2022) Ameliorative effect of ethoxylated chalcone-based MAO-B inhibitor on behavioural predictors of haloperidol-induced Parkinsonism in mice: evidence of its antioxidative role against Parkinson's diseases. Environ Sci Pollut Res Int 29(5):7271–7282. https://doi.org/10.1007/S11356-021-15955-3
Mardani Moghanaki M, Noormohammadi Z, Salahshourifar I, Mahdavi Hazaveh N (2022) MAOA-uVNTR variations in schizophrenia: case and control study. Bull Natl Res Cent 46(1):1–7. https://doi.org/10.1186/s42269-022-00951-5
Maršavelski A, Mavri J, Vianello R, Stare J (2022) Why monoamine oxidase B preferably metabolizes N-methylhistamine over histamine: evidence from the multiscale simulation of the rate-limiting step. Int J Mol Sci 23(3):1910. https://doi.org/10.3390/ijms23031910
Medina-Franco JL (2021) Grand challenges of computer-aided drug design: the road ahead. Front Drug Discov. https://doi.org/10.3389/FDDSV.2021.728551
Miar M, Shiroudi A, Pourshamsian K, Oliaey AR, Hatamjafari F (2021) Theoretical investigations on the HOMO–LUMO gap and global reactivity descriptor studies, natural bond orbital, and nucleus-independent chemical shifts analyses of 3-phenylbenzo [d] thiazole-2 (3 H)-imine and its para-substituted derivatives: solvent and substituent effects. J Chem Res 45(1–2):147–158. https://doi.org/10.1177/1747519820932091
Mondovì B, Finazzi Agrò A (1982) Structure and function of amine oxidase. Adv Exp Med Biol 148:141–153. https://doi.org/10.1007/978-1-4615-9281-5_12
Moya-Alvarado G, Yañez O, Morales N, González-González A, Areche C, Núñez MT, Fierro A, García-Beltrán O (2021) Coumarin-chalcone hybrids as inhibitors of MAO-B: biological activity and in silico studies. Molecules (Basel, Switzerland). https://doi.org/10.3390/MOLECULES26092430
Oh JM, Rangarajan TM, Chaudhary R, Gambacorta N, Nicolotti O, Kumar S, Mathew B, Kim H (2022) Aldoxime- and hydroxy-functionalized chalcones as highly potent and selective monoamine oxidase-B inhibitors. J Mol Struct 1250:131817. https://doi.org/10.1016/J.MOLSTRUC.2021.131817
Ouyang Y, Li J, Chen X, Fu X, Sun S, Wu Q (2021) Chalcone derivatives: role in anticancer therapy. Biomolecules. https://doi.org/10.3390/BIOM11060894
O'Boyle NM, Banck M, James CA, Morley C, Vandermeersch T, Hutchison GR (2011) Open babel: an open chemical toolbox. J Cheminform 3(10):33. https://doi.org/10.1186/1758-2946-3-33
Pettersen EF, Goddard TD, Huang CC, Couch GS, Greenblatt DM, Meng EC, Ferrin TE (2004) UCSF chimera—a visualization system for exploratory research and analysis. J Comput Chem 25(13):1605–1612. https://doi.org/10.1002/jcc.20084
Ramsay RR, Basile L, Maniquet A, Hagenow S, Pappalardo M, Saija MC, Bryant SD, Albreht A, Guccione S (2020) Parameters for irreversible inactivation of monoamine oxidase. Molecules. https://doi.org/10.3390/MOLECULES25245908
Rendić SP, Crouch RD, Guengerich FP (2022) Roles of selected non-P450 human oxidoreductase enzymes in protective and toxic effects of chemicals: review and compilation of reactions. Arch Toxicol. https://doi.org/10.1007/s00204-022-03304-3
Runge E, Gross EKU (1984) Density-functional theory for time-dependent systems. Phys Rev Lett 52(12):997. https://doi.org/10.1103/PhysRevLett.52.997
Sander T, Freyss J, Von Korff M, Rufener C (2015) DataWarrior: an open-source program for chemistry aware data visualization and analysis. J Chem Inf Model 55(2):460–473. https://doi.org/10.1021/CI500588J/ASSET/IMAGES/MEDIUM/CI-2014-00588J_0016.GIF
Schüller A, Hähnke V, Schneider G (2007) SmiLib v2.0: a java-based tool for rapid combinatorial library enumeration. QSAR Comb Sci 26(3):407–410. https://doi.org/10.1002/QSAR.200630101
Shih JC, Lan NC (1990) Structure and functional expression of cloned human liver MAO A and B. En Serotonin. Springer, Dordrecht, pp 61–65. https://doi.org/10.1007/978-94-009-1912-9_9
Shulman KI, Herrmann N, Walker SE (2013) Current place of monoamine oxidase inhibitors in the treatment of depression. CNS Drugs 27(10):789–797. https://doi.org/10.1007/S40263-013-0097-3
Tan QW, He LY, Zhang SS, He ZW, Liu WH, Zhang L, Guan LP, Wang SH (2022) Design, synthesis, and biological activity of chalcone analogs containing 4-phenylquinolin and benzohydrazide. Chem Biodivers 19(3):e202100610. https://doi.org/10.1002/CBDV.202100610
Trott O, Olson AJ (2010) AutoDock Vina: Improving the speed and accuracy of docking with a new scoring function, efficient optimization, and multithreading. J Comput Chem. https://doi.org/10.1002/jcc.21334
Vanommeslaeghe K, Hatcher E, Acharya C, Kundu S, Zhong S, Shim J, Darian E, Guvench O, Lopes P, Vorobyov I, MacKerell AD Jr (2010) CHARMM general force field (CGenFF): a force field for drug-like molecules compatible with the CHARMM all-atom additive biological force fields. J Comput Chem 31(4):671–690. https://doi.org/10.1002/jcc.21367.CHARMM
Weyesa A, Eswaramoorthy R, Melaku Y, Mulugeta E (2021) Antibacterial, docking, DFT and ADMET properties evaluation of chalcone-sulfonamide derivatives prepared using ZnO nanoparticle catalysis. Adv Appl Bioinform Chem AABC 14:133–144. https://doi.org/10.2147/AABC.S336450
Yang X, Wang Y, Byrne R, Schneider G, Yang S (2019) Concepts of artificial intelligence for computer-assisted drug discovery. Chem Rev 119(18):10520–10594. https://doi.org/10.1021/acs.chemrev.8b00728
Yelekçi K, Erdem SS (2023) Computational chemistry and molecular modeling of reversible MAO inhibitors. In: Binda C (eds) Monoamine oxidase. Methods in molecular biology, vol 2558. Humana, New York, NY. https://doi.org/10.1007/978-1-0716-2643-6_17
Yelekçi K, Karahan Ö, Toprakçı M (2007) Docking of novel reversible monoamine oxidase-B inhibitors: efficient prediction of ligand binding sites and estimation of inhibitors thermodynamic properties. J Neural Transm 114:725–732. https://doi.org/10.1007/s00702-007-0679-7
Yusufzai SK, Khan MS, Sulaiman O, Osman H, Lamjin DN (2018) Molecular docking studies of coumarin hybrids as potential acetylcholinesterase, butyrylcholinesterase, monoamine oxidase A/B and β-amyloid inhibitors for Alzheimer's disease. Chem Cent J. https://doi.org/10.1186/S13065-018-0497-Z
Zhao H, Lyu Y, Hu J, Li M, Sun W (2022) Decipher the molecular descriptors and mechanisms controlling sulfonamide adsorption onto mesoporous carbon: Density functional theory calculation and partial least-squares path modeling. J Hazard Mater. https://doi.org/10.1016/j.jhazmat.2022.129299

Publisher's Note